



**HAL**  
open science

# A Novel Partial Power Cascaded DC/DC Topology for CPV Application: A Theoretical Study

Philippe Camail, Christian Martin, Bruno Allard, Charles Joubert, Maxime Darnon, João Pedro F. Trovão

## ► To cite this version:

Philippe Camail, Christian Martin, Bruno Allard, Charles Joubert, Maxime Darnon, et al.. A Novel Partial Power Cascaded DC/DC Topology for CPV Application: A Theoretical Study. 2023 IEEE 14th International Conference on Power Electronics and Drive Systems (PEDS), IEEE, Aug 2023, Montreal, Canada. pp.1-6, 10.1109/PEDS57185.2023.10246548 . hal-04236853

**HAL Id: hal-04236853**

**<https://hal.science/hal-04236853>**

Submitted on 11 Oct 2023

**HAL** is a multi-disciplinary open access archive for the deposit and dissemination of scientific research documents, whether they are published or not. The documents may come from teaching and research institutions in France or abroad, or from public or private research centers.

L'archive ouverte pluridisciplinaire **HAL**, est destinée au dépôt et à la diffusion de documents scientifiques de niveau recherche, publiés ou non, émanant des établissements d'enseignement et de recherche français ou étrangers, des laboratoires publics ou privés.

# A Novel Partial Power Cascaded DC/DC Topology for CPV Application: A Theoretical Study

Philippe Camail Christian Martin  
Bruno Allard Charles Joubert  
Université de Lyon  
Ampère CNRS UMR 5005  
Université Claude Bernard Lyon 1  
INSA-Lyon, Ecole Centrale de Lyon  
69622 Villeurbanne, France

Maxime Darnon  
Laboratoire Nanotechnologies  
Nanosystèmes (LN2)  
CNRS IRL-3463 Institut Interdisciplinaire  
d'Innovation Technologique (3IT)  
Université de Sherbrooke  
Sherbrooke, Canada

João Pedro F. Trovão  
e-TESS Laboratory  
Dept. Electrical & Computer Engineering  
Université de Sherbrooke  
Sherbrooke, Canada

**Abstract**—This paper presents a novel partial power DC/DC topology for CPV applications. The context of the CPV requirements is first derived in terms of losses factor, and compared to traditional centralized topology. An additional cascaded DC/DC stage is then proposed. It consists of Delta Power Converters used for current independence cascaded with Partial Power Converters for string voltage independence. The theoretical explanation and example using realistic shading pattern are presented. Last, the increased yielded energy provided by the complete cascaded topology is shown.

**Index Terms**— CPV, DC/DC converter, DPC, PPC, flyback active clamp, cascaded topology, partial power processing

## I. INTRODUCTION

Concentrator photovoltaic (CPV) is an active field of development to increase the efficiency of photovoltaic conversion. At a panel level, prototype achieve photo-electric efficiencies up to 38.9% [1], which largely exceed capacities of traditional single junction silicon-based photovoltaic (PV) panels.

To do so, the main technological trend of CPV is the use of multijunction (usually three) of III-V semi-conductors. Due to the manufacturing complexity of such junctions, CPV cells size is reduced by the addition of a lens which concentrates the solar irradiance into a smaller surface. This lens-based solution limits the CPV panels to the use of Direct Normal Irradiance (DNI). A solar tracker, that aligns at every moment the sun irradiance with the focal point of the lens, becomes mandatory.

This leads to higher initial cost for CPV plants [2]. Hence, to reduce cost, industrials have chosen to directly transpose well used electrical solutions present in PV fields to extract energy. Indeed, most of CPV plants consists of panels put in series to form a string, and then those strings are placed in parallel to a common DC bus. This DC bus is then linked to the input of grid-tied inverter which manages both the conversion to the AC grid and the maximum power point tracking (MPPT) algorithm. Yet, this current solution shows limits in efficiency.

To address this limits, the addition of a conversion stage between the panels and the inverter is a well-known path. However complexifying the electrical energy capture approach must fulfill an economical balance. The paper details a simplified economical approach to evaluate the gain in efficiency

of an improvement in the DC/DC part of CPV power management. Test cases are presented to illustrate the methodology and discuss the potential benefit.

## II. ECONOMIC APPROACH

### A. Losses reduction

As mentioned, the panels-to-inverter structure has intrinsic losses. To quantify them, we introduce the performance ratio ( $PR$ ), which encompasses all the losses added by a given system. This  $PR$  ratio is then multiplied to the total energy at disposal, factoring the  $DNI$  received to obtain the energy that can be retrieved from the installation.

$$PR = \prod_{i=1}^I (1 - L_i) \quad (1)$$

The  $L_i$  (in %) are a generic way to represent both electrical and optical losses undergone by real CPV plants. The  $L_i$  parameters usually used by companies to determine the efficiency of their plants [3] are: Shading, Cell temperature, Lens temperature, DC wiring, Soiling, Mismatch, Inverter, AC wiring, Transformer, Auxiliary consumption and Unavailability. This list gives, for an industrial operation, a global  $PR$  between 0.8 and 0.9. In order to perform a quantitative analysis, we will use as reference value  $PR_{REF} = 0.8$ , without loss of generality regarding the subsequent conclusion. The interest of any work of improvement should aim at the decrease of one or more of the  $L_i$  parameters, to increase the performance factor, and thus on the total energy generated by the CPV (see (3)).

A promising solution to decrease some of these parameters is the diminution of the granularity of conversion to panel level. Indeed, some of the previous  $L_i$  parameters are due to the serie/parallel interconnection of panels and the centralized management of MPPT. It leads to power trade-offs that decrease the performance of the installation. By adding a conversion stage to the panel level, we can attenuate these trade-offs. This work focuses on reducing three  $L_i$  factors: shading losses, mismatch losses and unavailability.

1) *Shading Losses*: Shading losses are defined around two notions, losses by effective decrease of irradiance and losses caused by the disparity of MPPT strings voltages on the same tracker, related to the non-uniformity of shading patterns. It is evaluated by [4] as 3.5% ( $L_{shadREF}$ ) with current industrial connection. According to the same paper, by decreasing the granularity at the panel level, these losses decrease to 0.2% ( $L_{shad}$ ) (microinverters are used for this modeling, but our approach detailed in the following pages keeps the same panel level conversion).

2) *Mismatch losses*: Mismatch losses are related to the angular dispersion of a module with respect to its neighbors connected in series. In [5], authors define its impact around 4% ( $L_{mismREF}$ ), taking as a classical assumption a  $0.4^\circ$  angle change between the panels. The results presented in [6] claim that these losses are divided by 4 in the case of a conversion at the panel level. Therefore, we use  $L_{Mism} = 0.01$ .

3) *Unavailability losses*: The losses related to the unavailability of production ( $L_{unavailREF}$ ) due to maintenance are around 1% [3]. It is assumed that in the case of monitored converters (measurement of electrical parameters on panel), curative maintenance is no longer done blindly and that therefore, we can reduce downtime by half. We therefore take  $L_{unavail} = 0.005$ .

#### B. Addition of an intermediate DC stage

The addition of a DC/DC stage at panel level enables to keeps the industrially-proven installations (medium voltage high power grid tied inverters and related auxiliaries) and is synonym of a cost constrained choice. It also allows to keep others  $L_i$  unchanged. However, by adding an intermediate stage of conversion, we necessarily add conversion losses. To consider a specification for this conversion stage, we define a general DC efficiency that we vary from 90% to 99%. This translates to an added  $L_i$  ( $L_{DC}$ ) from 0.1 to 0.01 respectively.

To place this solution in context with the current market, the Levelized Cost of Energy (LCOE) metric is used. In the simplified *LCOE* model used (unless otherwise stated, all formulas are from [2]), it is possible to vary in input the efficiency of the conversion stage, the annual irradiance received, as well as the additional investment cost generated. For this last parameter, it is set to zero to have a minimum mandatory efficiency for the additional DC stage to prove economically useful. Indeed, if the LCOE of the added stage is superior to the LCOE of the existing installation, even with virtually no added cost, then we can conclude that it has no interest. The formula used is:

$$LCOE = \frac{LCC}{\sum_{n=1}^N \frac{E_{CPV}}{(1-d)^n}} \quad (2)$$

where  $LCC$  is the CPV system cost (in €) for a prospective life cycle  $N$  (in years),  $E_{CPV}$  is the annual energy obtained by the CPV system, and  $d$  the annual discount rate. The annual energy produced by the studied CPV system follows:

$$E_{CPV} = DNI_a \cdot P^* \cdot \frac{PR}{DNI_{CSOC}} \quad (3)$$

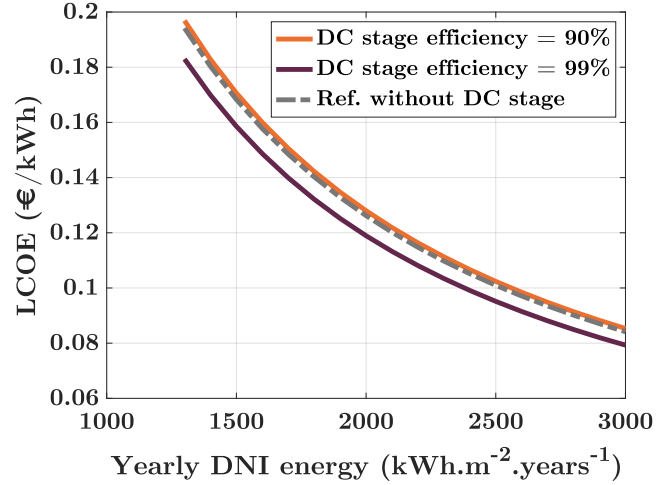


Fig. 1. LCOE in function of yearly energy received without added DC stage and with added DC stage

where  $DNI_a$  is the available energy per year by the direct normal irradiance,  $P^*$  is the power evaluated at the CSOC (Concentrator Standard Operating Conditions) available on the installation,  $DNI_{CSOC}$  the direct irradiance fixed at  $0.9\text{kW/m}^2$ .

Fig. 1 presents the LCOE versus yearly energy received considering the conditions described above. We can see a difference of up to  $0.9\text{c€/kWh}$  between the current CPV plants (in dotted gray) and an added conversion stage with 99% efficiency (in purple).

Nevertheless, with 90% efficiency (orange curve), we see that the calculated LCOE is higher than the current plants. More generally, this model indicates us that below 93% efficiency, an added DC/DC stage presents no economic advantage. This value represents therefore the minimum mandatory efficiency described above.

#### C. Opportunities

It is difficult to think in terms of absolute cost, predictive LCOE being related to a large number of economic assumptions and simplifications. It also heavily depends on the studied country. However, we saw that with high efficiency systems, few tens of cent per kWh could be saved. Recent worldwide assessment study [7] shows that the difference between LCOE of PV and CPV systems (as of 2020) is frequently below  $1\text{c€/kWh}$  in numerous countries (see [7] - Table A2). A highly efficient system can then theoretically permit a larger number of country and markets to consider deriving benefits from installing CPV plants when PV plants are affordable.

The new topology detailed below proposes to tackle both the cost (with a relatively low component count) and the efficiency (with partial power processing) challenges. It is the cascading of DPC converters with PPC. Both are well known for their extreme efficiencies (an average of 99% [8] for DPC and a peak of 96.6% [9] for PPC). Their simultaneous use is depicted in the following section.

### III. PRESENTATION OF TOPOLOGY

In order to reduce the three  $L_i$  parameters of interest, the chosen cascaded conversion solution is detailed in this section.

#### A. Delta Power Converter

The Delta Power Converter (DPC), also referred as Parallel Partial Processing Converter (P-PPC), is progressively used in led conversion, batteries management systems and solar installations [10]. In these domains, it allows to build up high DC voltage string by placing in series different units without the necessity of same-current sharing. For two units placed in series, the difference of currents between them is processed by the adjacent DPC converter.

In the context of PV study, if the total string voltage is the sum of the maximum power point voltage of each panel, the DPCs action (through the use of MPPT control) allow for each panel to work at their maximum power point current, which imply a yielded power calculation with the following equation:

$$P_{String} = \sum_{i=1}^{N_{panels}} P_{MPPi} \quad (4)$$

For  $n$  units,  $n-1$  DPCs are required to allow each unit to be current independent from one another. In this case, current processed by each DPC is a function of all the current mismatches present in the string of interest. In other words, even if the DPC managing two equal-current units is part of a larger string displaying current mismatches, it will process non-zero current. This leads to relatively high currents (and hence higher losses) processed by each DPC in the case of a series string consisting of numerous elements. In addition, the more units put in series, the higher the processed current. However, in the case of CPV, the already relatively high voltage of each unit (approx. 100V) in comparison to the targeted DC voltage (500V here), places us in the case of 4 CPV units for 3 DPC, which lowers this inter-dependency effect. In terms of power electronic systems, the most largely used DPC topology is based on a bi-directional, synchronous rectifier buck-boost architecture. The voltage rating is compatible with the use of Gallium Nitride (GaN) semiconductors in half bridge configuration.

For CPV, this means that mismatch losses related to the angular dispersion of a module with respect to its neighbors can be neglected, given the current independence. Concerning partial shading losses, if every cell of the module is still active (no cell sees  $0W/m^2$ ), this effect of maximum power point finding still holds.

However, if some cells see no irradiance at all, and that the pattern differs from one string to another, the simple parallel interconnection of strings with DPC cannot overcome the voltage difference [10]. In this situation, the use of an additional converter is necessary.

#### B. Partial Power Converter

Due to the numerous amounts of bypass diodes present in CPV modules, partial shading patterns lead to important

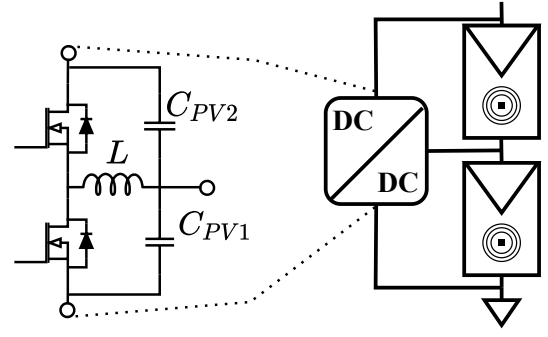


Fig. 2. DPC buck boost topology

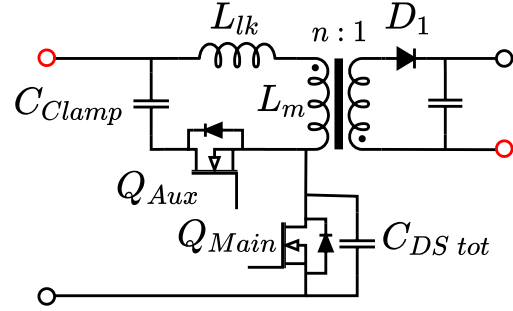


Fig. 3. Flyback active clamp topology

differences of voltages between strings. Usually, with the traditional approach of CPV in series and strings in parallel, a global MPPT algorithm decreases/increases the DC bus voltage to a trade-off voltage. This likely results in whole irradiated panels or sometimes strings disconnected to the benefit of more irradiated ones. Ensuring a way to overcome this problem is particularly critical as a commonly shading pattern in CPV plants is inter-tracker shading [6], which systematically occurs at dawn and twilight. This is the role of the second stage of this cascaded topology.

The Partial Power Converter (PPC) consists of a flyback active clamp (FBAC) [11] in input parallel output series. This way of plugging is depicted at the top of Fig. 5. The partial power link implies that the low side output of the converter is set to the high side voltage of the input, placing its output effectively in series with the source (here, a string of panels). By doing so, the current used by the secondary of the FBAC is directly collected from the high side of the input, hence the partial power processing. The ratio of partial power management depends on the voltage gain of the converter between the input (the voltage of the string) and its output (the difference between the input and the DC bus voltage). The closer the input voltage is to the DC bus voltage, the less power is processed through the converter. Therefore, it allows an overall better efficiency (the losses are only applied to the processed power) and a smaller power rating than the equivalent converter without the partial power processing feature. A fully detailed design of this converter applied for the CPV requirements can be found at [9]. The advantage of

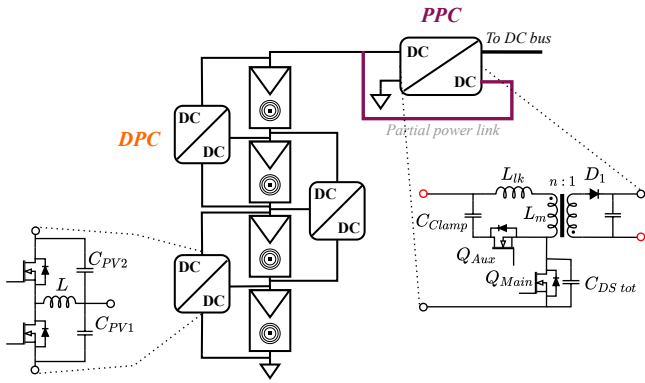


Fig. 4. Proposed cascaded partial power conversion topology

FBAC topology resides in its low component count (active and passive) and its ability to perform soft switching throughout most of its requirement in terms of power and voltage, if designed with care.

In addition, if the input voltage is close enough to the total DC bus voltage, the FBAC can be disconnected (by stopping switching orders to its primary side) and the string is directly connected to the DC bus by the intermediary of its secondary diode. Dealing with DC currents, the presence of the secondary inductor can be neglected. This feature is also interesting in the case of converter disfunction. Indeed, if an active switch is lost in open circuit configuration, then the converter can be entirely bypassed the same way.

### C. Complete cascaded stage

The complete topology proposed in this paper is represented in Fig. 4. It consists of the addition of the two stages presented above: DPCs for current independence between panels, and PPCs for voltage independence between strings. They both implement MPPT algorithms, and leading the inverter to only regulate the DC bus voltage to a constant operating point. This allows the inverter to work at an optimal DC where its efficiency is maximum.

However, control and communication are two concerns to take into account to ensure the simultaneous use of these topologies working with the same power source [12].

Concerning control, it should be pointed at that DPCs and PPCs control objectives are neither redundant nor coupled if designed carefully. The firsts control the current of each of their assigned panels by adjusting the voltage ratio between their input and their output. In fact, DPCs cumulated action within a string cannot increase nor decrease the total voltage of this string. This total voltage regulation is devolved to the PPC. Their action is decoupled if the frequency of the MPPT (and of the regulation itself) performed by DPC is fast enough compared with the MPPT of the downstream converter [8].

This point is also valid concerning communication, so following this requirement, there is no need for data exchange between DPCs and their PPC. In addition, some work has been already achieved in recent years [13], [12] to mitigate the need of communication only to neighbor-to-neighbor data

exchange. This cancels the need for a more complex centralized controller.

## IV. THEORETICAL RESULTS

### A. Mismatch pattern

In order to check the relevance of the proposed topology, our study is synthesized in one irradiance pattern that encompasses the partial shadow mismatches of interest. Two strings of four panels in series are used, with different irradiances. String n°1 consists of (from top to bottom, as seen in fig. 5) one CPV panel fully irradiated at  $1000\text{W/m}^2$ , one fully at  $800\text{W/m}^2$ , one fully at  $300\text{W/m}^2$ , and a last one which sees on its first half  $300\text{W/m}^2$  and on its second half no irradiance ( $0\text{W/m}^2$ ). String n°2 consists of fully irradiated panels at  $1000\text{W/m}^2$ ,  $1000\text{W/m}^2$ ,  $800\text{W/m}^2$  and  $300\text{W/m}^2$  respectively. Figure 5 recalls the I-V curves of the adjacent panels. The considered temperature of operation is  $25^\circ\text{C}$ , and bypass diode reverse voltage is taken into account. Three cases are depicted:

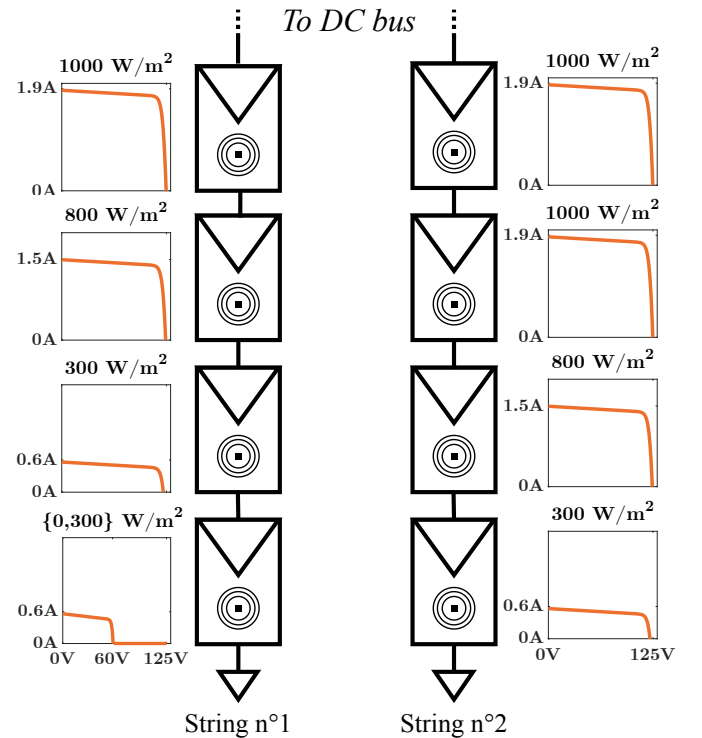


Fig. 5. Two strings considered for this study; each panel has its I-V curve depicted next to it (all I-V curves share the same Voltage/Current scale to ease comparison)

- Case 1: String n°1 and string n°2 are placed in parallel without intermediate conversion stage (current industrial solution).
- Case 2: 3 lossless DPCs are added to string n°1 and string n°2, both then placed in parallel.
- Case 3: a PPC is added to each DPC-equipped string to represent the full solution.

The results presented in the following section are mathematically generated using I-V curves of a CPV panel at different

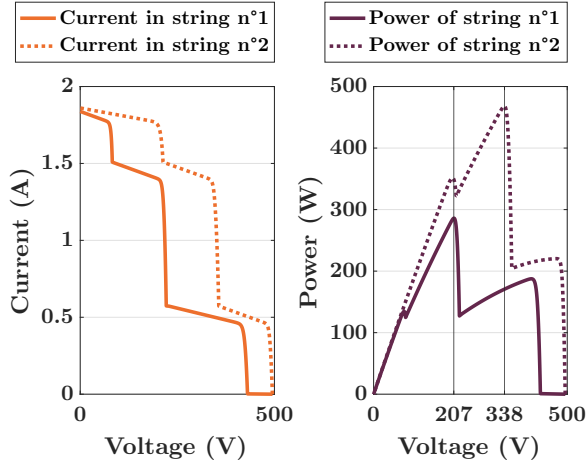


Fig. 6. I-V curves (left) of string n°1 (solid) and string n°2 (dotted), and corresponding P-V curves (right) for case n°1

irradiances. The 5 parameters model was derived using method depicted in [14].

## B. Results

1) *Case 1: Current industrial solution:* In this case, strings n°1 and n°2 are placed directly in parallel on the DC bus. Fig. 6 shows the I-V curves of each string. We can note 3 current drops with increasing voltages. They are representing each time when the most irradiated panels are forced to work at the next lower current, due to the “turn on” of a new less irradiated panel. For each string, the maximum power point is found at 207V and 338V respectively. These two voltage values are found again in the Fig. 7 depicting the I-V and the P-V curves of the complete set up (as seen by the theoretical inverter downstream). Here, these two voltages represent the two highest local maxima. The inverter performing the MPPT algorithm will choose (given the ability to systematically find the global maximum) the 338V voltage point.

It means in this case that two panels will be bypassed (the less irradiated of each string), and four panels will work at suboptimal currents (the two most irradiated of each string). The resulting power extracted is 37.5% less than the total power in presence. It can be noted that the multiple local maxima displayed in fig. 7 adds difficulty to the completion of the centralized MPPT algorithm. More advanced techniques than traditional Perturb & Observe (P&O) standard algorithm are mandatory.

2) *Case 2: Addition of DPC:* DPC are added to the two strings. The total voltage of the strings is still controlled by the DC side of the inverter, as said previously. Under the assumption that the MPPT of the DPCs is realized faster than the one of the inverter, (a few tens times faster), the I-V patterns of each string are seen by the inverter as *smoothened*. To sum up, only one maximum is found at each string, as seen in fig. 8. This results in only two local maxima for the total P-V curve presented in fig. 9. The global maximum is set

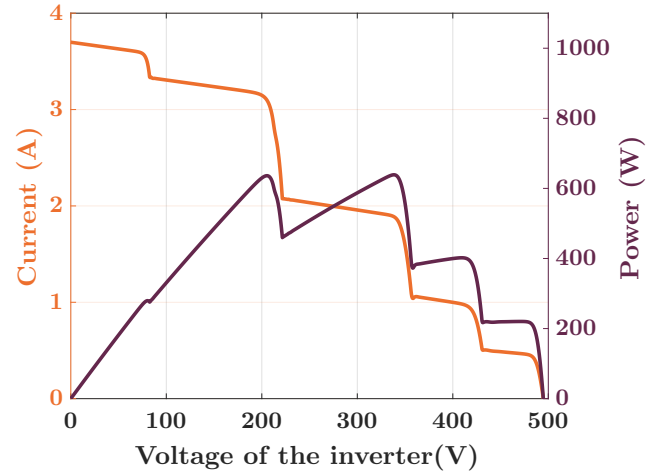


Fig. 7. Total I-V (orange) and P-V (purple) curves as seen by the central inverter for case n°1

at 407V. At this voltage value, all panels of string n°1 work approximately at their maximum power points, and all panels of string n°2 are working at above 90% of their capacity (see Table I). Considering lossless converters, a panel-to-inverter efficiency of 94.5% is displayed. Still, the inverter-side MPPT has to perform a trade-off by decreasing the voltage of its DC side, affecting the ability of string n°2 to work at full power.

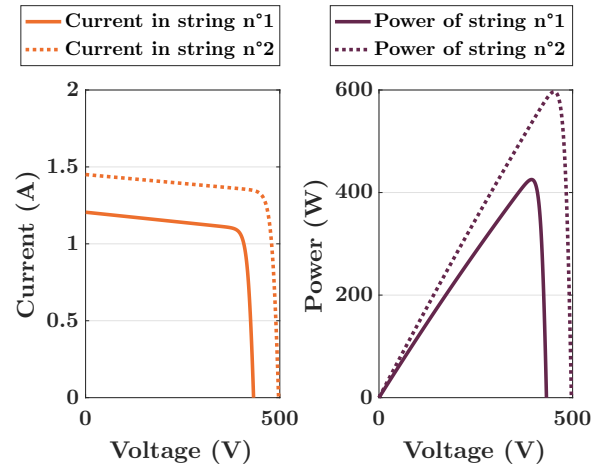


Fig. 8. I-V curves (left) of string n°1 (solid) and string n°2 (dotted), and corresponding P-V curves (right) for case n°2

3) *Case 3: Proposed cascaded topology:* To solve this last issue, string voltage independence is given through the addition of PPC for each string. In this case, the I-V and P-V curves presented in Fig.9 still hold, but the decoupled voltage allow to extract the maximum theoretical power by setting each string at their global optimal voltage.

As we can note in the third line of Table I, the collected power is the same as the total power at disposal. In order to get a more realistic idea of the yielded power, a last line

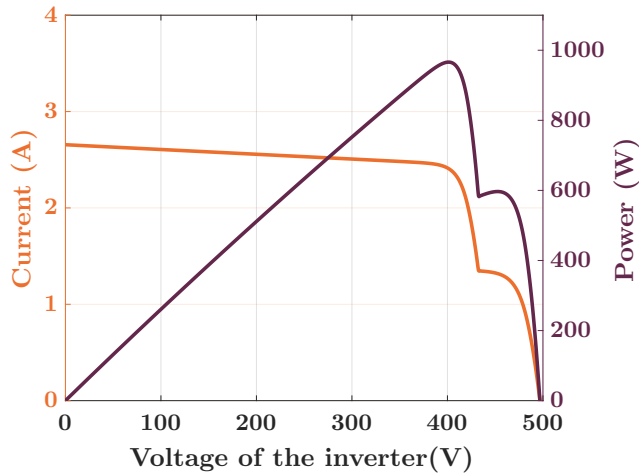


Fig. 9. Total I-V (orange) and P-V (purple) curves as seen by the central inverter for case n°2

with losses has been added in the table. It factors in efficiency results present in [8] and [9].

We can see that compared to the current industrial solution depicted by case n°1, case n°3 (with losses) allows a very significant increase in the total power at disposal. The transition from 62.5% to 95.6% power yielding brings forward the interest of our cascaded topology.

TABLE I  
POWER RESULTS

|  | Power collected in string n°1 | Power collected in string n°2 | Total power available |
|--|-------------------------------|-------------------------------|-----------------------|
| Case n°1                                   | 171W (40.2%)                  | 468W (78.3%)                  | 639W (62.5%)          |
| Case n°2                                   | 422W (99%)                    | 544W (91.1%)                  | 966W (94.5%)          |
| Case n°3                                   | 425W (100%)                   | 597W (100%)                   | 1022W (100%)          |
| Case n°3<br>(With losses from [8] and [9]) | 406W (95.5%)                  | 571W (95.6%)                  | 977W (95.6%)          |

## V. CONCLUSION

In this paper, a simplified economical study has been achieved to evaluate the conditions of a gain in efficiency of an extra DC/DC stage. A condition of at least 93% efficiency has been drawn. This stage is considered to be added to an already existing centralized inverter configuration for CPV. A novel topology aiming to match these efficiency/cost conditions is presented. It is theoretically tested against a realistic, heavily mismatching shadowing pattern. Later work will include real time simulations of this topology, with a focus on angular mismatch of CPV panels. The aim of this simulation will be to derive an accurate loss calculation to include to the Performance Ratio presented in this work.

## REFERENCES

[1] M. A. Green, E. D. Dunlop, J. Hohl-Ebinger, M. Yoshita, N. Kopydakis, and X. Hao, "Solar cell efficiency tables (Version

58)," *Progress in Photovoltaics: Research and Applications*, vol. 29, no. 7, pp. 657–667, Jul. 2021. [Online]. Available: <https://onlinelibrary.wiley.com/doi/10.1002/pip.3444>

[2] C. Algora and I. Rey-Stolle, Eds., *Handbook of concentrator photovoltaic technology*. Hoboken: John Wiley & Sons Inc, 2016.

[3] T. Gerstmaier, T. Zech, M. Röttger, C. Braun, and A. Gombert, "Large-scale and long-term CPV Power Plant Field Results," Aix-les-Bains, France, 2015, p. 030002. [Online]. Available: <http://aip.scitation.org/doi/abs/10.1063/1.4931506>

[4] P. Rodrigo, "Balancing the shading impact in utility-scale dual-axis tracking concentrator photovoltaic power plants," *Energy*, vol. 210, p. 118490, Nov. 2020. [Online]. Available: <https://linkinghub.elsevier.com/retrieve/pii/S036054422031598X>

[5] Y. S. Kim and R. Winston, "Power conversion in concentrating photovoltaic systems: central, string, and micro-inverters: Power conversion in CPV systems," *Progress in Photovoltaics: Research and Applications*, vol. 22, no. 9, pp. 984–992, Sep. 2014. [Online]. Available: <http://doi.wiley.com/10.1002/pip.2317>

[6] P. Rodrigo, R. Velázquez, E. F. Fernández, F. Almonacid, and P. Pérez-Higueras, "Analysis of electrical mismatches in high-concentrator photovoltaic power plants with distributed inverter configurations," *Energy*, vol. 107, pp. 374–387, Jul. 2016. [Online]. Available: <https://linkinghub.elsevier.com/retrieve/pii/S0360544216304455>

[7] D. Talavera, J. Ferrer-Rodríguez, P. Pérez-Higueras, J. Terrados, and E. Fernández, "A worldwide assessment of levelised cost of electricity of HCPV systems," *Energy Conversion and Management*, vol. 127, pp. 679–692, Nov. 2016. [Online]. Available: <https://linkinghub.elsevier.com/retrieve/pii/S0196890416308536>

[8] C. Schaefer and J. T. Stauth, "Multilevel Power Point Tracking for Partial Power Processing Photovoltaic Converters," *IEEE Journal of Emerging and Selected Topics in Power Electronics*, vol. 2, no. 4, pp. 859–869, Dec. 2014. [Online]. Available: <http://ieeexplore.ieee.org/document/6842654/>

[9] P. Camail, C. Martin, B. Allard, C. Joubert, M. Darnon, and J. P. Trovao, "Application of DC/DC Partial Power Conversion to Concentrator Photovoltaics," in *IECON 2022 – 48th Annual Conference of the IEEE Industrial Electronics Society*. Brussels, Belgium: IEEE, Oct. 2022, pp. 1–6. [Online]. Available: <https://ieeexplore.ieee.org/document/9968818/>

[10] O. Khan and W. Xiao, "Review and qualitative analysis of submodule-level distributed power electronic solutions in PV power systems," *Renewable and Sustainable Energy Reviews*, vol. 76, pp. 516–528, Sep. 2017. [Online]. Available: <https://linkinghub.elsevier.com/retrieve/pii/S1364032117304094>

[11] R. Perrin, N. Quentin, B. Allard, C. Martin, and M. Ali, "High-Temperature GaN Active-Clamp Flyback Converter With Resonant Operation Mode," *IEEE Journal of Emerging and Selected Topics in Power Electronics*, vol. 4, no. 3, pp. 1077–1085, Sep. 2016. [Online]. Available: <http://ieeexplore.ieee.org/document/7437383/>

[12] S. Qin and R. C. Pilawa-Podgurski, "Sub-module differential power processing for photovoltaic applications," in *2013 Twenty-Eighth Annual IEEE Applied Power Electronics Conference and Exposition (APEC)*. Long Beach, CA, USA: IEEE, Mar. 2013, pp. 101–108. [Online]. Available: <http://ieeexplore.ieee.org/document/6520193/>

[13] M. O. Badawy, S. M. Bose, and Y. Sozer, "A Novel Differential Power Processing Architecture for a Partially Shaded PV String Using Distributed Control," *IEEE Transactions on Industry Applications*, vol. 57, no. 2, pp. 1725–1735, Mar. 2021. [Online]. Available: <https://ieeexplore.ieee.org/document/9302874/>

[14] D. Chan and J. Phang, "Analytical methods for the extraction of solar-cell single- and double-diode model parameters from I-V characteristics," *IEEE Transactions on Electron Devices*, vol. 34, no. 2, pp. 286–293, Feb. 1987. [Online]. Available: <http://ieeexplore.ieee.org/document/1486631/>